

The combination of temozolomide-irinotecan regresses a doxorubicin-resistant patient-derived orthotopic xenograft (PDOX) nude-mouse model of recurrent Ewing's sarcoma with a FUS-ERG fusion and CDKN2A deletion: Direction for third-line patient therapy

Kentaro Miyake^{1,2,3}, Takashi Murakami^{1,2,3}, Tasuku Kiyuna^{1,2}, Kentaro Igarashi^{1,2}, Kei Kawaguchi^{1,2}, Masuyo Miyake^{1,2,3}, Yunfeng Li⁵, Scott D. Nelson⁵, Sarah M. Dry⁵, Michael Bouvet², Irmina A. Elliott⁶, Tara A. Russell⁶, Arun S. Singh⁴, Mark A. Eckardt⁷, Yukihiko Hiroshima³, Masashi Momiyama³, Ryusei Matsuyama³, Takashi Chishima³, Itaru Endo³, Fritz C. Eilber⁶ and Robert M. Hoffman^{1,2}

¹AntiCancer Inc., San Diego, CA, USA

²Department of Surgery, University of California, San Diego, CA, USA

³Department of Gastroenterological Surgery, Yokohama City University Graduate School of Medicine, Yokohama, Japan

⁴Division of Hematology-Oncology, University of California, Los Angeles, CA, USA

⁵Department of Pathology, University of California, Los Angeles, CA, USA

⁶Division of Surgical Oncology, University of California, Los Angeles, CA, USA

⁷Department of Surgery, Yale School of Medicine, New Haven, CT, USA

Correspondence to: Robert M. Hoffman, **email:** all@anticancer.com
Fritz C. Eilber, **email:** fceilber@mednet.ucla.edu

Keywords: Ewing's sarcoma, patient-derived orthotopic xenograft, irinotecan, temozolomide, third-line chemotherapy

Received: July 14, 2017

Accepted: July 23, 2017

Published: September 08, 2017

Copyright: Miyake et al. This is an open-access article distributed under the terms of the Creative Commons Attribution License 3.0 (CC BY 3.0), which permits unrestricted use, distribution, and reproduction in any medium, provided the original author and source are credited.

ABSTRACT

The aim of the present study was to determine the usefulness of a patient-derived orthotopic xenograft (PDOX) nude-mouse model of a doxorubicin-resistant metastatic Ewing's sarcoma, with a unique combination of a FUS-ERG fusion and CDKN2A deletion, to identify effective drugs for third-line chemotherapy of the patient. Our previous study showed that cyclin-dependent kinase 4/6 (CDK4/6) and insulin-like growth factor-1 receptor (IGF-1R) inhibitors were effective on the Ewing's sarcoma PDOX, but not doxorubicin, similar to the patient's resistance to doxorubicin. The results of the previous PDOX study were successfully used for second-line therapy of the patient. In the present study, the PDOX mice established with the Ewing's sarcoma in the right chest wall were randomized into 5 groups when the tumor volume reached 60 mm³: untreated control; gemcitabine combined with docetaxel (intraperitoneal [i.p.] injection, weekly, for 2 weeks); irinotecan combined with temozolomide (irinotecan: i.p. injection; temozolomide: oral administration, daily, for 2 weeks); pazopanib (oral administration, daily, for 2 weeks); yonnelis (intravenous injection, weekly, for 2 weeks). All mice were sacrificed on day 15. Body weight and tumor volume were assessed 2 times per week. Tumor weight was measured after sacrifice. Irinotecan combined with temozolomide was the most effective regimen compared to the untreated control group (p=0.022). Gemcitabine combined with docetaxel was also effective (p=0.026). Pazopanib and yonnelis did

not have significant efficacy compared to the untreated control (p=0.130, p=0.818). These results could be obtained within two months after the physician's request and were used for third-line therapy of the patient.

INTRODUCTION

Ewing's sarcoma (ES) is a rare and aggressive disease that mostly affects children and teenagers [1, 2]. The development of multi-agent chemotherapy has improved outcome [3–6], but is not effective for ES patients with metastasis [7]. Furthermore, the heterogeneity of ES makes the treatment decisions much more complicated [8, 9].

We previously established a patient-derived orthotopic xenograft (PDOX) models of a rare case of ES with both a *FUG-ERG* fusion [10, 11] and a loss of the *CDKN2A*. Previously, we reported that a CDK4/6 inhibitor and insulin-like growth factor-1 receptor (IGF-1R) inhibitor were effective in the ES PDOX model [12]. The PDOX tumor was resistant to doxorubicin (DOX) as was the patient [12]. ES recurred in the bone marrow of the patient 19 months after primary tumor resection and DOX treatment. Based on the PDOX results, an IGF-1R inhibitor was used successfully as a second line therapy for the bone marrow recurrence in the patient. The patient's physician requested a subsequent PDOX test and the results of the present study were used for treatment of remaining organ metastasis.

RESULTS AND DISCUSSION

The site of implantation of the ES in the nude mice is shown in Figure 1. The treatment schema is illustrated in Figure 2. The time-course change of the tumor volume ratio is shown in Figure 3. The combination of irinotecan (IRT) with temozolomide (TEM) was most effective, and showed significant tumor regression compared to the untreated control group on day 15 ($p < 0.001$). There was also a significant difference between the untreated control group and the mice treated with the combination of gemcitabine (GEM) with docetaxel (DOC) on day 15 ($p = 0.001$). Pazopanib (PAZ) suppressed the tumor growth significantly on day 15 ($p = 0.001$). Yondelis (YON) did not significantly suppress tumor growth ($p = 0.342$). Final relative tumor volume ratios on day 15 compared to day 1 were as follows: untreated control group (G1) (3.13 ± 0.5); combination with GEM with DOC (G2) (1.47 ± 0.47); combination with IRT with TEM (G3) (0.41 ± 0.11); PAZ (G4) (1.87 ± 0.35); YON (G5) (2.64 ± 0.35). The 0.41 relative tumor volume of the IRT-TEM group indicates tumor regression, which is important for clinical translation of the efficacy of IRT-TEM for the patient [13].

There was no significant difference in body weight on day 1 and day 15 between the 5 groups (Figure 4)

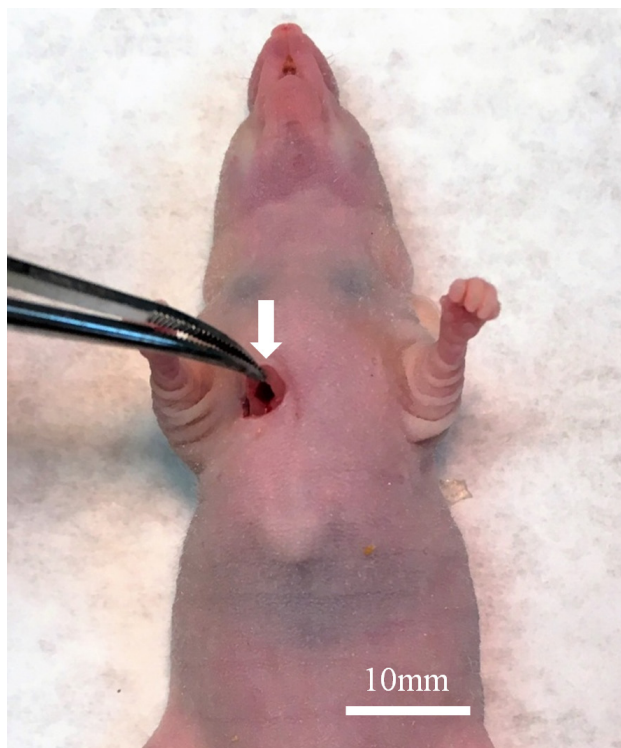


Figure 1: Surgical orthotopic implantation of Ewing's sarcoma (ES) tumor. A space between the pectoral muscle (white arrow) and intercostal muscle was made in the right chest wall of nude mice for orthotopic implantation of the ES tumor.

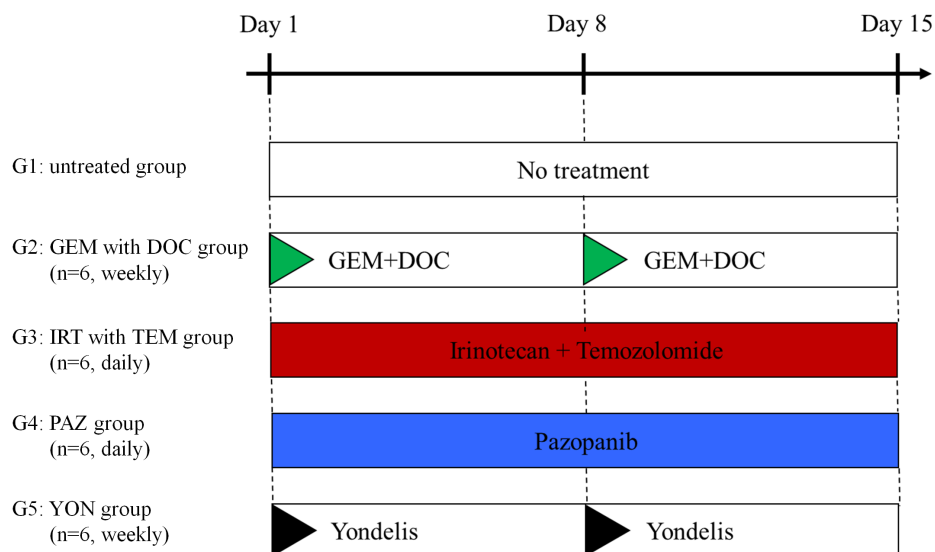


Figure 2: Treatment protocol for ES PDOX. G1: untreated control; G2: combination treatment with GEM + DOC (GEM: intraperitoneal [i.p.], 100 mg/kg, weekly, 2 weeks, DOC: i.p., 20 mg/kg, weekly, 2 weeks); G3: combination treatment with IRT + TEM (IRT: i.p., 4 mg/kg, daily, 2 weeks, TEM: oral [p.o.], 25 mg/kg, daily, 2 weeks); G4: PAZ (p.o., 100 mg/kg, daily, 2 weeks); G5: YON (intravenous [i.v.], 0.15 mg/kg, weekly, 2 weeks). Each group consisted of n=6 mice. All mice were sacrificed on day 15. GEM=gemcitabine; DOC=docetaxel; IRT=irinotecan; TEM=temozolomide.

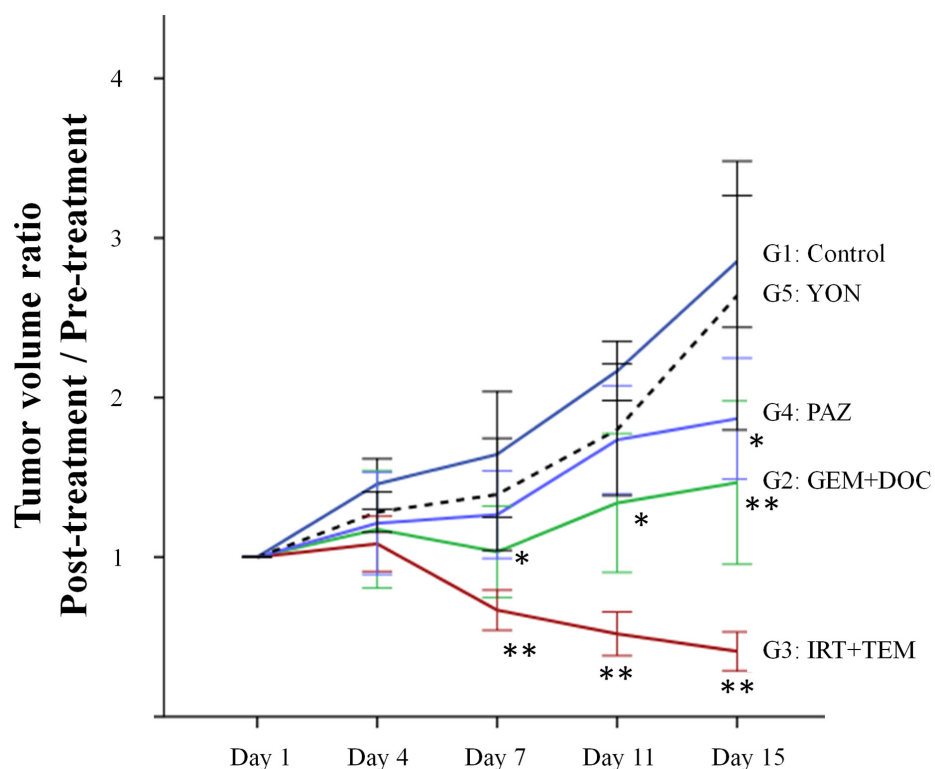


Figure 3: Time course of tumor volume ratio in treated mice compared to untreated control. Line graphs indicate tumor volume ratio (post-treatment volume / pre-treatment volume) on each tumor-measurement day. IRT combined with TEM regressed tumor growth significantly compared to the untreated control group on day 7, 11 and 15 ($p < 0.001$). There was also a significant difference between the untreated control group and the mice treated with the combination of GEM with DOC group on day 7, 11, and 15 ($p = 0.004$, $p = 0.002$, and $p = 0.001$), respectively. PAZ suppressed the tumor growth significantly on day 15 ($p = 0.001$). * $P < 0.01$, ** $P < 0.001$ compared to untreated group. Error bars: ± 1 SD.

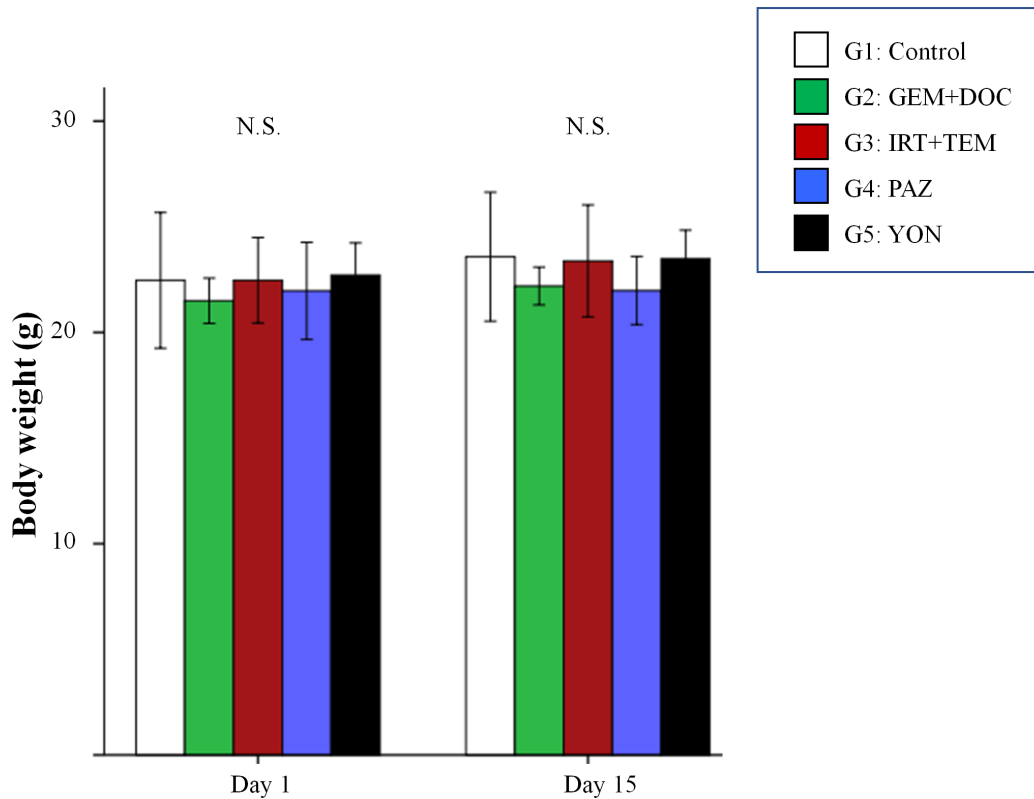


Figure 4: Body weight of treated versus untreated mice. Bar graphs indicate body weight in each group on day 1 and 15. No significant difference was observed between any group. Error bars: ± 1 SD.

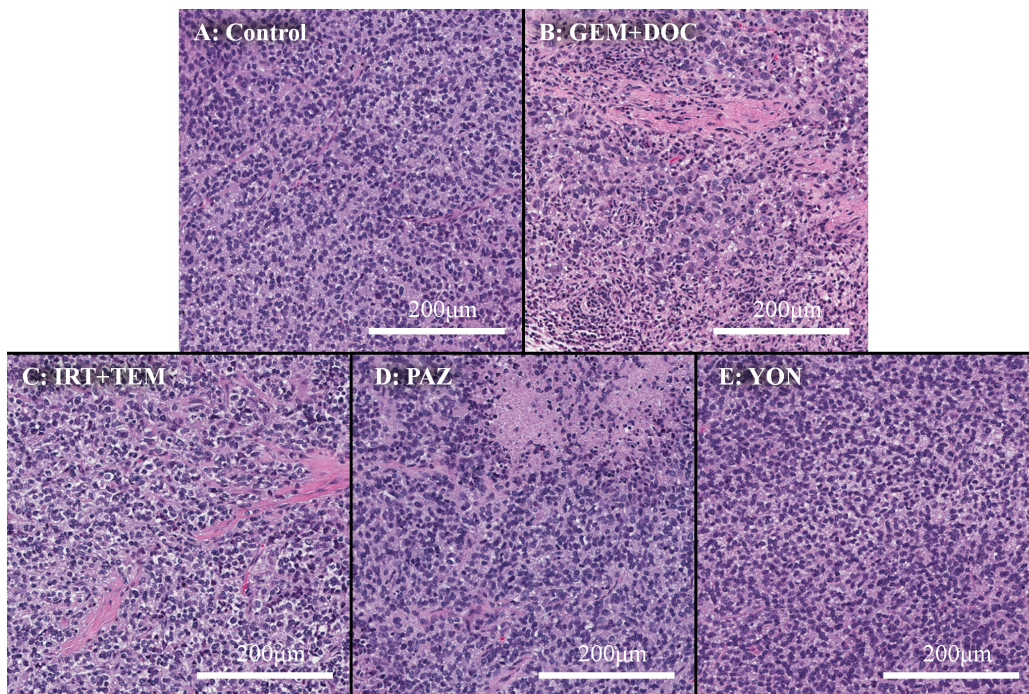


Figure 5: Histopathology. (A) Hematoxylin and eosin (H&E) staining of the untreated PDOX tumor. (B) H&E staining of a tumor treated with the combination of GEM and DOC. (C) H&E staining of a tumor treated with the combination of IRT and TEM. (D) H&E staining of a tumor treated with PAZ. (E) H&E staining a tumor treated with YON. Necrosis was observed in all treatment groups other than YON.

suggesting there was no acute toxicity due to any of the treatments.

Hematoxylin and eosin (H&E)-staining of tumor tissue sections showed necrosis due to treatment with all drugs except YON (Figure 5). The previously-established ES PDOX model had similar histological findings compared to the original patient's tumor [12].

Toward the goal of precision personalized oncology, our laboratory pioneered the patient-derived orthotopic xenograft (PDOX) nude mouse model with the technique of surgical orthotopic implantation (SOI), including pancreatic [14–18], breast [19], ovarian [20], lung [21], cervical [22, 23], colon [24–26], and stomach cancer [27], sarcoma [12, 28–37] and melanoma [38–42].

The heterogeneity of ES makes individualized therapy particularly pertinent for this disease and the PDOX model can play an important role in achieving this goal.

Based on the efficacy of an IGF-1R inhibitor in the ES PDOX model [12], a compassionate-use investigational new drug (IND) approval was obtained from the U.S. Food and Drug Administration (FDA) for second-line treatment of the ES patient with an IGF-1R inhibitor, which resulted in clearance of the ES from the patient's bone marrow (Eilber, F.C, et al., unpublished results), thereby allowing subsequent cytotoxic chemotherapy to be administered for third line therapy. We obtained the present results within only 2 months from receiving the physician's request using the ES PDOX model, in time for third-line therapy guidance. These results thereby demonstrate an important clinical use of the PDOX model.

The ES PDOX was also shown to be sensitive to experimental therapeutics including recombinant methioninase [43] and *Salmonella typhimurium* A1-R [34].

Previously-developed concepts and strategies of highly-selective tumor targeting can take advantage of molecular targeting of tumors, including tissue-selective therapy which focuses on unique differences between normal and tumor tissues [44–49].

CONCLUSIONS

An effective drug combination was identified using the PDOX model for recurrent Ewing's sarcoma within a time frame to design a treatment strategy for third line therapy of the patient, demonstrating the power of the PDOX model for individualized therapy.

MATERIALS AND METHODS

Mice

Athymic *nu/nu* female nude mice (AntiCancer Inc., San Diego, CA, USA), 4–6 weeks old, were used in this study. Animals were housed in a barrier facility on a high efficiency particulate arrestance (HEPA)-filtered rack

under standard conditions of 12-hour light/dark cycles. The animals were fed an autoclaved laboratory rodent diet [12]. All animal studies were conducted with an AntiCancer Institutional Animal Care and Use Committee (IACUC)-protocol specifically approved for this study and in accordance with the principals and procedures outlined in the National Institutes of Health Guide for the Care and Use of Animals under Assurance Number A3873-1. In order to minimize any suffering of the animals the use of anesthesia and analgesics were used for all surgical experiments. Animals were anesthetized by subcutaneous injection of a 0.02 ml solution of 20 mg/kg ketamine, 15.2 mg/kg xylazine, and 0.48 mg/kg acepromazine maleate. The response of animals during surgery was monitored to ensure adequate depth of anesthesia. The animals were observed on a daily basis and humanely sacrificed by CO₂ inhalation when they met the following humane endpoint criteria: severe tumor burden (more than 20 mm in diameter), prostration, significant body weight loss, difficulty breathing, rotational motion and body temperature drop.

Previous establishment of the ES PDOX model

The ES tumor recurred in the right chest wall of the patient [12]. The patient received neoadjuvant multidrug chemotherapy using doxorubicin, vincristine, and cyclophosphamide. Then, curative intent surgery was performed in the Department of Surgery, University of California, Los Angeles, USA (UCLA) and a portion of the tumor was previously used for establishment of a PDOX model in the right chest wall of nude mice [12]. Informed consent was previously obtained from the patient, and this study was approved by the Institutional Review Board of UCLA. Fresh tumor was brought to AntiCancer Inc. from the UCLA Hospital [12]. The ES PDOX was established by implantation between the pectoral muscle and intercostal muscle in the right chest wall of nude mice [12] (Figure 1).

Treatment protocol for the ES PDOX model

The PDOX mice were randomized into 5 groups before tumor volume reached 60 mm³: G1: untreated control; G2: gemcitabine (GEM) combined with docetaxel (DOC) (GEM: i.p., 100 mg/kg, weekly, 2 weeks, DOC: i.p., 20 mg/kg, weekly, 2 weeks); G3: irinotecan (IRT) with temozolomide (TEM) (IRT: i.p., 4 mg/kg, daily, 2 weeks, TEM: p.o., 25 mg/kg, daily, 2 weeks); G4: pazopanib (PAZ) (p.o., 100 mg/kg, daily, 2 weeks); G5: yondelis (YON) (i.v., 0.15 mg/kg, weekly, 2 weeks) (Figure 2). Drug dosages were determined using previous reports (13-16). Tumor size and body weight were measured 2 times a week. Tumor volume was calculated with the following formula: tumor volume (mm³) = length (mm)

x width (mm) x width (mm) x ½ [12]. After 2 weeks, all mice were sacrificed.

Histological examination

Fresh tumor samples were fixed in 10% formalin and embedded in paraffin before sectioning and staining. Tissue sections (5 µm) were deparaffinized in xylene and rehydrated in an ethanol series. Hematoxylin and eosin (H&E) staining was performed according to standard protocols. Histological examination was performed with a BHS System Microscope (Olympus Corporation, Tokyo, Japan). Images were acquired with INFINITY ANALYZE software (Lumenera Corporation, Ottawa, Canada) [12].

Statistical analysis

All statistical analyses were performed with the Statistical Package for the Social Sciences for Windows software version 22.0 (IBM Corp., Armonk, NY, USA). Significant differences for continuous variables were determined using the Mann-Whitney U test. Line graphs show the median and error bars indicate ± standard deviation. A probability value of $P \leq 0.05$ was defined as statistically-significant [12].

ACKNOWLEDGMENT/GRANT SUPPORT

This study was supported in part by National Cancer Institute Grant CA 213649.

DEDICATION

This paper is dedicated to the memory of A. R. Moossa, M.D., and Sun Lee, M.D.

CONFLICTS OF INTEREST

K.M., T.M., T.K., K.I., K.K. M.M., and R.M.H. are unsalaried associates of AntiCancer Inc. There are no other competing financial interests.

REFERENCES

1. Balamuth NJ, Womer RB. Ewing's sarcoma. *Lancet Oncol.* 2010; 11:184–92.
2. Biswas B, Bakhshi S. Management of Ewing sarcoma family of tumors: current scenario and unmet need. *World J Orthop.* 2016; 7:527–38.
3. Rosen G, Wollner N, Tan C, Wu SJ, Hajdu SI, Cham W, D'Angio GJ, Murphy ML. Proceedings: disease-free survival in children with Ewing's sarcoma treated with radiation therapy and adjuvant four-drug sequential chemotherapy. *Cancer.* 1974; 33:384–93.
4. Jaffe N, Paed D, Traggis D, Salian S, Cassady JR. Improved outlook for Ewing's sarcoma with combination chemotherapy (vincristine, actinomycin D and cyclophosphamide) and radiation therapy. *Cancer.* 1976; 38:1925–30.
5. Burgert EO Jr, Nesbit ME, Garnsey LA, Gehan EA, Herrmann J, Vietti TJ, Cangir A, Tefft M, Evans R, Thomas P. Multimodal therapy for the management of nonpelvic, localized Ewing's sarcoma of bone: intergroup study IESS-II. *J Clin Oncol.* 1990; 8:1514–24.
6. Smith MA, Ungerleider RS, Horowitz ME, Simon R. Influence of doxorubicin dose intensity on response and outcome for patients with osteogenic sarcoma and Ewing's sarcoma. *J Natl Cancer Inst.* 1991; 83:1460–70.
7. Biswas B, Rastogi S, Khan SA, Shukla NK, Deo SV, Agarwala S, Sharma DN, Thulkar S, Vishnubhatla S, Pathania S, Bakhshi S. Hypoalbuminaemia is an independent predictor of poor outcome in metastatic Ewing's sarcoma family of tumours: a single institutional experience of 150 cases treated with uniform chemotherapy protocol. *Clin Oncol (R Coll Radiol).* 2014; 26:722–29.
8. Llombart-Bosch A, Machado I, Navarro S, Bertoni F, Bacchini P, Alberghini M, Karzeladze A, Savelov N, Petrov S, Alvarado-Cabrero I, Mihaila D, Terrier P, Lopez-Guerrero JA, Picci P. Histological heterogeneity of Ewing's sarcoma/PNET: an immunohistochemical analysis of 415 genetically confirmed cases with clinical support. *Virchows Arch.* 2009; 455:397–411.
9. DNA methylation analysis shows epigenetic heterogeneity in Ewing sarcoma. *Cancer Discov.* 2017; 7:347.
10. Chen S, Deniz K, Sung YS, Zhang L, Dry S, Antonescu CR. Ewing sarcoma with ERG gene rearrangements: A molecular study focusing on the prevalence of FUS-ERG and common pitfalls in detecting EWSR1-ERG fusions by FISH. *Genes Chromosomes Cancer.* 2016; 55:340–49.
11. Shing DC, McMullan DJ, Roberts P, Smith K, Chin SF, Nicholson J, Tillman RM, Ramani P, Cullinane C, Coleman N. FUS/ERG gene fusions in Ewing's tumors. *Cancer Res.* 2003; 63:4568–76.
12. Murakami T, Singh AS, Kiyuna T, Dry SM, Li Y, James AW, Igarashi K, Kawaguchi K, DeLong JC, Zhang Y, Hiroshima Y, Russell T, Eckardt MA, et al. Effective molecular targeting of CDK4/6 and IGF-1R in a rare FUS-ERG fusion CDKN2A-deletion doxorubicin-resistant Ewing's sarcoma patient-derived orthotopic xenograft (PDOX) nude-mouse model. *Oncotarget.* 2016; 7:47556–64. <https://doi.org/10.18632/oncotarget.9879>
13. Kurmasheva RT, Houghton PJ. Chapter 11, The use of pediatric patient-derived xenografts for identifying novel agents and combinations. In: Patient-Derived Mouse Models of Cancer. Hoffman, R.M., ed. *Molecular and Translational Medicine.* Series eds., Coleman, W.B., Tsongalis, G.J. ISSN: 2197-7852.

14. Hiroshima Y, Zhang Y, Murakami T, Maawy A, Miwa S, Yamamoto M, Yano S, Sato S, Momiyama M, Mori R, Matsuyama R, Chishima T, Tanaka K, et al. Efficacy of tumor-targeting *Salmonella typhimurium* A1-R in combination with anti-angiogenesis therapy on a pancreatic cancer patient-derived orthotopic xenograft (PDOX) and cell line mouse models. *Oncotarget*. 2014; 5:12346–57. <https://doi.org/10.18632/oncotarget.2641>
15. Fu X, Guadagni F, Hoffman RM. A metastatic nude-mouse model of human pancreatic cancer constructed orthotopically with histologically intact patient specimens. *Proc Natl Acad Sci USA*. 1992; 89:5645–49.
16. Hiroshima Y, Maawy A, Zhang Y, Murakami T, Momiyama M, Mori R, Matsuyama R, Katz MH, Fleming JB, Chishima T, Tanaka K, Ichikawa Y, Endo I, et al. Metastatic recurrence in a pancreatic cancer patient derived orthotopic xenograft (PDOX) nude mouse model is inhibited by neoadjuvant chemotherapy in combination with fluorescence-guided surgery with an anti-CA 19-9-conjugated fluorophore. *PLoS One*. 2014; 9:e114310.
17. Hiroshima Y, Maawy AA, Katz MH, Fleming JB, Bouvet M, Endo I, Hoffman RM. Selective efficacy of zoledronic acid on metastasis in a patient-derived orthotopic xenograft (PDOX) nude-mouse model of human pancreatic cancer. *J Surg Oncol*. 2015; 111:311–15.
18. Kawaguchi K, Igarashi K, Murakami T, Kiyuna T, Lwin TM, Hwang HK, DeLong JC, Clary BM, Bouvet M, Unno M, Hoffman RM. MEK inhibitors cobimetinib and trametinib, regressed a gemcitabine-resistant pancreatic-cancer patient-derived orthotopic xenograft (PDOX). *Oncotarget*. 2017; 8:47490-47496. <https://doi.org/10.18632/oncotarget.17667>
19. Fu X, Le P, Hoffman RM. A metastatic orthotopic-transplant nude-mouse model of human patient breast cancer. *Anticancer Res*. 1993; 13:901–04.
20. Fu X, Hoffman RM. Human ovarian carcinoma metastatic models constructed in nude mice by orthotopic transplantation of histologically-intact patient specimens. *Anticancer Res*. 1993; 13:283–86.
21. Wang X, Fu X, Hoffman RM. A new patient-like metastatic model of human lung cancer constructed orthotopically with intact tissue via thoracotomy in immunodeficient mice. *Int J Cancer*. 1992; 51:992–95.
22. Hiroshima Y, Zhang Y, Zhang N, Maawy A, Mii S, Yamamoto M, Uehara F, Miwa S, Yano S, Murakami T, Momiyama M, Chishima T, Tanaka K, et al. Establishment of a patient-derived orthotopic Xenograft (PDOX) model of HER-2-positive cervical cancer expressing the clinical metastatic pattern. *PLoS One*. 2015; 10:e0117417.
23. Murakami T, Kiyuna T, Kawaguchi K, Igarashi K, Singh AS, Hiroshima Y, Zhang Y, Zhao M, Miyake K, Nelson SD, Dry SM, Li Y, DeLong JC, et al. The irony of highly-effective bacterial therapy of a patient-derived orthotopic xenograft (PDOX) model of Ewing's sarcoma, which was blocked by Ewing himself 80 years ago. *Cell Cycle*. 2017; 16:1046–52.
24. Fu XY, Besterman JM, Monosov A, Hoffman RM. Models of human metastatic colon cancer in nude mice orthotopically constructed by using histologically intact patient specimens. *Proc Natl Acad Sci USA*. 1991; 88:9345–49.
25. Metildi CA, Kaushal S, Luiken GA, Talamini MA, Hoffman RM, Bouvet M. Fluorescently labeled chimeric anti-CEA antibody improves detection and resection of human colon cancer in a patient-derived orthotopic xenograft (PDOX) nude mouse model. *J Surg Oncol*. 2014; 109:451–58.
26. Hiroshima Y, Maawy A, Metildi CA, Zhang Y, Uehara F, Miwa S, Yano S, Sato S, Murakami T, Momiyama M, Chishima T, Tanaka K, Bouvet M, et al. Successful fluorescence-guided surgery on human colon cancer patient-derived orthotopic xenograft mouse models using a fluorophore-conjugated anti-CEA antibody and a portable imaging system. *J Laparoendosc Adv Surg Tech A*. 2014; 24:241–47.
27. Furukawa T, Kubota T, Watanabe M, Kitajima M, Hoffman RM. Orthotopic transplantation of histologically intact clinical specimens of stomach cancer to nude mice: correlation of metastatic sites in mouse and individual patient donors. *Int J Cancer*. 1993; 53:608–12.
28. Murakami T, DeLong J, Eilber FC, Zhao M, Zhang Y, Zhang N, Singh A, Russell T, Deng S, Reynoso J, Quan C, Hiroshima Y, Matsuyama R, et al. Tumor-targeting *Salmonella typhimurium* A1-R in combination with doxorubicin eradicate soft tissue sarcoma in a patient-derived orthotopic xenograft (PDOX) model. *Oncotarget*. 2016; 7:12783–90. <https://doi.org/10.18632/oncotarget.7226>
29. Hiroshima Y, Zhao M, Zhang Y, Zhang N, Maawy A, Murakami T, Mii S, Uehara F, Yamamoto M, Miwa S, Yano S, Momiyama M, Mori R, et al. Tumor-targeting *Salmonella typhimurium* A1-R arrests a chemo-resistant patient soft-tissue sarcoma in nude mice. *PLoS One*. 2015; 10:e0134324.
30. Kiyuna T, Murakami T, Tome Y, Kawaguchi K, Igarashi K, Zhang Y, Zhao M, Li Y, Bouvet M, Kanaya F, Singh A, Dry S, Eilber FC, Hoffman RM. High efficacy of tumor-targeting *Salmonella typhimurium* A1-R on a doxorubicin- and dactolisib-resistant follicular dendritic-cell sarcoma in a patient-derived orthotopic xenograft PDOX nude mouse model. *Oncotarget*. 2016; 7:33046–54. <https://doi.org/10.18632/oncotarget.8848>
31. Hiroshima Y, Zhang Y, Zhang N, Uehara F, Maawy A, Murakami T, Mii S, Yamamoto M, Miwa S, Yano S, Momiyama M, Mori R, Matsuyama R, et al. Patient-derived orthotopic xenograft (PDOX) nude mouse model of soft-tissue sarcoma more closely mimics the patient behavior in contrast to the subcutaneous ectopic model. *Anticancer Res*. 2015; 35:697–701.

32. Kawaguchi K, Igarashi K, Murakami T, Kiyuna T, Nelson SD, Dry SM, Li Y, Russell TA, Singh AS, Chmielowski B, Unno M, Eilber FC, Hoffman RM. Combination of gemcitabine and docetaxel regresses both gastric leiomyosarcoma proliferation and invasion in an imageable patient-derived orthotopic xenograft (iPDOX) model. *Cell Cycle*. 2017; 16:1063–69.
33. Igarashi K, Kawaguchi K, Murakami T, Kiyuna T, Miyake K, Nelson SD, Dry SM, Li Y, Yanagawa J, Russell TA, Singh AS, Yamamoto N, Hayashi K, et al. Intra-arterial administration of tumor-targeting Salmonella typhimurium A1-R regresses a cisplatin-resistant relapsed osteosarcoma in a patient-derived orthotopic xenograft (PDOX) mouse model. *Cell Cycle*. 2017; 16:1164–70.
34. Murakami T, Igarashi K, Kawaguchi K, Kiyuna T, Zhang Y, Zhao M, Hiroshima Y, Nelson SD, Dry SM, Li Y, Yanagawa J, Russell T, Federman N, et al. Tumor-targeting Salmonella typhimurium A1-R regresses an osteosarcoma in a patient-derived xenograft model resistant to a molecular-targeting drug. *Oncotarget*. 2017; 8:8035-8042. <https://doi.org/10.18632/oncotarget.14040>
35. Igarashi K, Kawaguchi K, Kiyuna T, Murakami T, Miwa S, Nelson SD, Dry SM, Li Y, Singh A, Kimura H, Hayashi K, Yamamoto N, Tsuchiya H, et al. Patient-derived orthotopic xenograft (PDOX) mouse model of adult rhabdomyosarcoma invades and recurs after resection in contrast to the subcutaneous ectopic model. *Cell Cycle*. 2017; 16:91–94.
36. Igarashi K, Kawaguchi K, Murakami T, Kiyuna T, Miyake K, Singh AS, Nelson SD, Dry SM, Li Y, Yamamoto N, Hayashi K, Kimura H, Miwa S, et al. High efficacy of pazopanib on an undifferentiated spindle-cell sarcoma resistant to first-line therapy is identified with a patient-derived orthotopic xenograft (PDOX) nude mouse model. *J Cell Biochem*. 2017; 118:2739–43.
37. Igarashi K, Kawaguchi K, Kiyuna T, Murakami T, Miwa S, Nelson SD, Dry SM, Li Y, Singh A, Kimura H, Hayashi K, Yamamoto N, Tsuchiya H, et al. Temozolomide combined with irinotecan caused regression in an adult pleomorphic rhabdomyosarcoma patient-derived orthotopic xenograft (PDOX) nude-mouse model. *Oncotarget*. 2017; 8:75874-75880. <https://doi.org/10.18632/oncotarget.16548>.
38. Yamamoto M, Zhao M, Hiroshima Y, Zhang Y, Shurell E, Eilber F. C, Bouvet M, Noda M, Hoffman RM. Efficacy of tumor-targeting Salmonella typhimurium A1-R on a melanoma patient-derived orthotopic xenograft (PDOX) nude-mouse model. *PLoS One*. 2016; 11:e0160882.
39. Kawaguchi K, Murakami T, Chmielowski B, Igarashi K, Kiyuna T, Unno M, Nelson SD, Russell TA, Dry SM, Li Y, Eilber FC, Hoffman RM. Vemurafenib-resistant BRAF-V600E-mutated melanoma is regressed by MEK-targeting drug trametinib, but not cobimetinib in a patient-derived orthotopic xenograft (PDOX) mouse model. *Oncotarget*. 2016; 7:71737-71743. <https://doi.org/10.18632/oncotarget.12328>
40. Kawaguchi K, Igarashi K, Murakami T, Chmielowski B, Kiyuna T, Zhao M, Zhang Y, Singh A, Unno M, Nelson SD, Russell TA, Dry SM, Li Y, et al. Tumor-targeting Salmonella typhimurium A1-R combined with temozolomide regresses malignant melanoma with a BRAF-V600E mutation in a patient-derived orthotopic xenograft (PDOX) model. *Oncotarget*. 2016; 7:85929-85936. <https://doi.org/10.18632/oncotarget.13231>
41. Kawaguchi K, Igarashi K, Murakami T, Kiyuna T, Zhao M, Zhang Y, Nelson SD, Russell TA, Dry SM, Singh AS, Chmielowski B, Li Y, Unno M, et al. Salmonella typhimurium A1-R targeting of a chemotherapy-resistant BRAF-V600E melanoma in a patient-derived orthotopic xenograft (PDOX) model is enhanced in combination with either vemurafenib or temozolomide. *Cell Cycle*. 2017; 16:1288–94.
42. Kawaguchi K, Igarashi K, Murakami T, Zhao M, Zhang Y, Chmielowski B, Kiyuna T, Nelson SD, Russell TA, Dry SM, Li Y, Unno M, Eilber FC, Hoffman RM. Tumor-targeting Salmonella typhimurium A1-R sensitizes melanoma with a BRAF-V600E mutation to vemurafenib in a patient-derived orthotopic xenograft (PDOX) nude mouse model. *J Cell Biochem*. 2017; 118:2314–19.
43. Murakami T, Li S, Han Q, Tan Y, Kiyuna T, Igarashi K, Kawaguchi K, Hwang HK, Miyake K, Singh AS, Nelson SD, Dry SM, Li Y, et al. Recombinant methioninase effectively targets a Ewing's sarcoma in a patient-derived orthotopic xenograft (PDOX) nude-mouse model. *Oncotarget*. 2017; 8:35630-35638. <https://doi.org/10.18632/oncotarget.15823>
44. Blagosklonny MV. Matching targets for selective cancer therapy. *Drug Discov Today*. 2003; 8:1104–07.
45. Blagosklonny MV. Teratogens as anti-cancer drugs. *Cell Cycle*. 2005; 4:1518–21.
46. Blagosklonny MV. Treatment with inhibitors of caspases, that are substrates of drug transporters, selectively permits chemotherapy-induced apoptosis in multidrug-resistant cells but protects normal cells. *Leukemia*. 2001; 15:936–41.
47. Blagosklonny MV. Target for cancer therapy: proliferating cells or stem cells. *Leukemia*. 2006; 20:385–91.
48. Apontes P, Leontieva OV, Demidenko ZN, Li F, Blagosklonny MV. Exploring long-term protection of normal human fibroblasts and epithelial cells from chemotherapy in cell culture. *Oncotarget*. 2011; 2:222–33. <https://doi.org/10.18632/oncotarget.248>
49. Blagosklonny MV. Tissue-selective therapy of cancer. *Br J Cancer*. 2003; 89:1147–51.